REPORT DOCUMENTATION PAGE

Form Approved OMB No. 0704-0188

1. AGENCY USE ONLY (Leave blank)	2. REPORT DATE	3. REPORT TYPE AND DATES COVERED
	29 Oct 99	Final Report

4. TITLE AND SUBTITLE	5. FUNDING NUMBERS
"Discovery of Leonid Meteoric Cloud"	F6256298M9194
6. AUTHOR(S) R. Nakamura, Y. Fujii, M. Ishiguro, K. Morishige, S. Yokogawa, and T. Mukai	
7. PERFORMING ORGANIZATION NAME(S) AND ADDRESS(ES) Information Processing Center, Kobe University Rokko-dai 1-1, Nada, Kobe 657-8501 Japan Graduate School of Science and Technology and Graduate School of Science	8. PERFORMING ORGANIZATION REPORT NUMBER N/A
9. SPONSORING/MONITORING AGENCY NAME(S) AND ADDRESS(ES) AOARD UNIT 45002 APO AP 96337-5002	10. SPONSORING/MONITORING AGENCY REPORT NUMBER AOARD98-4008

11. SUPPLEMENTARY NOTES

12a. DISTRIBUTION/AVAILABILITY STATEMENT	12b. DISTRIBUTION CODE
Approved for public release; distribution is unlimited.	A

13. ABSTRACT (Maximum 200 words)

A meteoric cloud is a faint glow of sunlight scattered by the small meteoroids in the trail along a parent comet's orbit. Here we report the first detection of the meteoric cloud associated with the Leonid meteor stream. Our photometric observations, performed on Mauna Kea, Hawaii, reveal the cloud as a local enhancement in sky brightness during the meteor shower in 1998. The radius of the trail, deduced from the spatial extent of the cloud, is approximately 0.01 astronomical unit and is consistent with the duration of the meteor stream activities. The brightness of the cloud is approximately 2 – 3 percent of the background zodiacal light and cannot be explained by the simple model calculations based on the zenith hourly rate and population index of the meteor stream activities in 1998. If the typical size of the cloud particles in 10 *um* and the albedo is 0.1, the brightness is transformed into a number density of 1.5e-16/*cm3*.

19991109 004

14. SUBJECT TERMS	15. NUMBER OF PAGES
Meteoroids, Meteor Stream, Photometric, Zenith Hourly Rate, Production Index	12
	16. PRICE CODE N/A

17. SECURITY CLASSIFICATION OF REPORT	18. SECURITY CLASSIFICATION OF THIS PAGE	19, SECURITY CLASSIFICATION OF ABSTRACT	20. LIMITATION OF ABSTRACT
UNCLASSIFIED	UNCLASSIFIED	UNCLASSIFIED	UL

NSN 7540-01-280-5500

Standard Form 298 (Rev. 2-89)
Prescribed by ANSI Std. 239-18
298-102

Final report for the grant from US AOARD

Discovery of Leonid Meteoric Cloud

R. Nakamura[1], Y. Fujii[2], M. Ishiguro[2], K. Morishige[3], S.Yokogawa[3] and T. Mukai[2]

[1] Information Processing Center, Kobe Univ., Kobe 657-8501, Japan

[2]Graduate School of Science and Technology, Kobe Univ., Kobe 657-8501, Japan

[3]Graduate School of Science, Univ. of Tokyo, Tokyo 113-8654, Japan

ABSTRACT

A meteoric cloud is the faint glow of sunlight scattered by the small meteoroids in the trail along a parent comet's orbit. Here we report the first detection of the meteoric cloud associated with the Leonid meteor stream. Our photometric observations, performed on Mauna Kea, Hawaii, reveal the cloud as a local enhancement in sky brightness during the meteor shower in 1998. The radius of the trail, deduced from the spatial extent of the cloud, is approximately 0.01 astronomical unit and is consistent with the duration of the meteor stream activities. The brightness of the cloud is approximately 2 $\sim$ 3 percent of the background zodiacal light, and cannot be explained by simple model calculations based on the zenith hourly rate and population index of the meteor stream activities in 1998 [1]. If the typical size of cloud particles is 10 μm and the albedo is 0.1, the brightness is transformed into a number density of 1.5e-16 $/cm^3$.

A cometary dust tail consists of small dust particles, blown out by solar radiation pressure forces, while larger dust particles form a tube-like structure around the parent comet's orbit. If a comet comes close enough to the Earth's orbit, the entry of dust particles into the atmosphere can be observed as a meteor stream and such dust particles are called meteoroids. We expect outburst activity of a meteor stream just after the return of the parent comet, since they are thought to originate from relatively young meteoroids in the dense and narrow trail behind the parent comet, as discovered by the Infrared Astronomical Satellite [2]. On the other hand, there is another kind of dust trail that includes the whole orbit of the parent comet and causes the annual meteor stream activities. The formation processes of such trails are not well understood, because the models include many unknown parameters, such as the comet's past activities, size dependence in the dust ejection velocity [3] and the combined effect of the planets' gravity and solar radiation pressure forces on the dusts orbital evolution [4]. If we observe the trail from the inside, sunlight scattered by the meteoroids should yield a dim glow in the sky, i.e. a meteoric cloud. While no convincing detection has previously been reported [5], ground-based observations with a wide-angle lens and a CCD camera have the potential to detect such faint and diffuse structures, as demonstrated by the recent identification of asteroidal dust bands [6].

There are two advantages to detecting a meteoric cloud during a significant meteor shower. These are

the high spatial density of meteoroids and the long line of sight in the tangential direction of the trail. Leonid is the most famous meteor stream, because of its spectacular outbursts [7]. Historical records imply that an outburst occurs when the distance between the Earth and the descending node of the parent comet P/Tempel-Tuttle is smaller than 0.01 astronomical unit (AU), and the Earth crosses the cometary orbital plane after the perihelion passage [8]. These conditions were fully met in 1998, and we actually observed a meteor shower with a maximum zenith hourly rate (ZHR) of more than 300 [1]. Figure 1 shows the appearance of a model trail along the orbit of P/Tempel-Tuttle when the Earth was located in the middle of the trail. On the basis of the duration of meteor activities, we assume that the cross section of the trail is a circle with a 0.01 AU radius. Due to the almost retrograde orbit of P/Tempel-Tuttle, the model cloud is close to the radiant, and extends approximately 4° on the sky for lines of sight longer than 0.3 AU. Using a wide-angle lens (Sigma 24mm lens, F=2.8) attached to a cooled CCD camera (Mutoh CV-16), we made photometric observations of this region of the sky between 1^h35^m and $5^h05^m(HST)$ on 17th November 1998, atop Mauna Kea, Hawaii, at an altitude of 4200 meters. The angular resolution and the field of view are 2.50'/pixel and 32° × 21° respectively. The transmittance spectrum of the filter is designed to agree with the broadest window of visible airglow lines between Hg at 435 nm and OI at 557.7 nm. The exposure time was set to 3 minutes, and the temperature of the CCD chip was kept at - $30^\circ C$. In order to check the dark and readout noise during these observations, 49 dark frames were obtained throughout the night. The calibration frames for flat fielding were taken by the same instrument inside the integrating sphere in the National Institute of Polar Research (NIPR), Tokyo, Japan. For detailed analysis, we used the last frame, taken just before dawn, because it had the smallest zenith angle. The rest frames allow us to estimate the optical depth $\tau(z)$ through photometry of standard stars with changing zenith angles. From photometry of solar analog stars, it has been found that 1 ADU on our system is equal to 3.41 $S_{10\odot}$ (= 1.28 10^{-8}W/m^2/sr/μm at 500nm).

After removing stars, we applied a Sivan-Gorray smoothing filer [9] to obtain the sky brightness. On a moonless night, observed sky brightness (I_{obs}) consists of light from several different sources, *i.e.* zodiacal light (I_{ZL}) including the contribution from the meteoric cloud, airglow from the upper atmosphere (I_{AG}), integrated starlight of unresolved stars (I_{ISL}), and light scattered by the Earth's atmosphere (I_{sca}). That is,

$$I_{obs} = (I_{ZL} + I_{AG} + I_{ISL}) \cdot exp(-\tau_{eff}(z)) + I_{sca} \tag{1}$$

where $\tau_{eff}(z)$ denotes the effective optical depth for the extinction of diffuse light sources at zenith distance z. We estimate $\tau_{eff}(z)$ by using the empirical formula $\tau_{eff}(z) \simeq 0.75\ \tau(z)$ [10]. I_{ISL} is calculated by interpolating Pioneer's data cited in Leinert *et al.* [11], and I_{sca} comes from the formulae by Dumont [12]. The resulting image, after these reduction procedures, is shown in the larger panel of Figure 2. The zenith angle dependence of I_{AG} is described by the van Rhijn function [13], but normalization must be done at the zenith. Furthermore, we must subtract the smooth component of the zodiacal light to extract the faint meteoric cloud. We have constructed a model of zodiacal light in which the spatial distribution function of interplanetary dust particles and the scattering function were taken from Kelsall et al. [14] and Hong [15], respectively. The tilt of the symmetry plane of the zodiacal light and I_{AG} at the zenith were determined simultaneously by a simplex method, so that the combination gave an optimal fit to the off-cloud regions in the observed data. The regions with large zenith angles were excluded from this fitting procedure in advance. Finally, we subtracted I_{AG} and I_{ZL} from the background image and superimposed the resulting structure as the contours in Figure 2. The peak intensity of the meteoric cloud is approximately 4.5 $S_{10\odot}$, while I_{ZL} amounts to approximately 200 $S_{10\odot}$ at the center of the frame, and I_{AG} at the zenith is 90 $S_{10\odot}$. The interval between the contour lines is 0.5 $S_{10\odot}$ and the fluctuation of sky brightness, caused mainly by photon noise and dark current, is approximately 1 $S_{10\odot}$. Although the shape is rather elongated in the orbital plane of P/Tempel-Tuttle, possibly due to anisotropy in the ejection velocities, the location and extent of the meteoric cloud are consistent with the prediction shown in Figure 1. The lunar sodium tail induced by the meteor shower [16] cannot be responsible for this structure, since our filter cuts out the neutral sodium emission at 589.1 nm, as noted before. If a star is bright enough to have a blooming tail, it produces a halo, as shown in the smaller panel of Figure 2. The region around the contour map, however, is free from halos, because stars of similar magnitude to those in the contour map show no indication of halos. In order to further check the possibility that the diffuse structure resulted from unknown diffuse sources, either beyond the solar system or within the Earth's atmosphere, on 20th December 1998 we performed the same observations as in November, and applied the same reduction procedures. As the diffuse structure found on 17th November was not detected, the connection with the Leonid meteor activities was established.

Wu and Williams [17] have shown that the outburst activities of the Leonid meteor stream are caused by relatively young dust particles that have completed only a few orbits since ejection from the nucleus. On the other hand, small and young meteoroids cannot contribute to the cloud, due to radiation pressure forces, as shown below. For simplicity, we consider the meteoroids released at perihelion and neglect the

effect of ejection velocity. Then, a meteoroid's eccentricity and perihelion distance are given by [18]

$$e = (1-\beta)^{-1}(e_p + \beta) \tag{2}$$

$$q = q_p(1+e_p)(1+e)^{-1}(1-\beta)^{-1} \tag{3}$$

where β represents the ratio of the radiation pressure force to the gravitational force acting on the meteoroid, and q_p and e_p denote the perihelion distance and the eccentricity of parent comets respectively. Using these equations, we calculated meteoroids' orbital periods and found that meteoroids with β larger than 0.001 cannot return to the vicinity of the Earth's orbit along with P/Tempel-Tuttle. If the meteoroids consist of astronomical silicate, $\beta = 0.001$ corresponds to a radius of roughly 100 μm. Assuming a simple power-law size distribution of meteoroids with this lower limit, we can estimate the brightness of the meteoric cloud as follows. The mass M and magnitude m of a meteoroid are assumed to obey a simple power-law as $M(m) = M(0) * 10^{-\alpha * m}$, where $M(0)$ is the mass of a zero magnitude meteor. On the other hand, the meteor flux $n(m)$ and the population index χ are determined as $n(m) = n(0) * \chi^m$ by visual observations. The values of $n(0)$ and $M(0)$ for Leonid can be found in Jenniskens [19]. The two equations give the mass-distribution function of the meteoroids as

$$n(M) = \kappa * M^{\gamma} \tag{4}$$

where

$$\kappa = -ln10 * \alpha * n(0) * M(0)^{log\chi/\alpha} \quad \text{and} \quad \gamma = -(1 + log\chi/\alpha) \tag{5}$$

If this power-law covers the whole size range, we can obtain the total scattering cross section by size integration. As long as $\gamma \leq 5/3$, the total scattering cross section is dominated by the lower limit of meteoroid size and is insensitive to the upper limit. The upper limit is set to 10 cm throughout this paper. When meteoroids are distributed uniformly in the trail, the mean volume scattering function of the meteoroids inside the trail is given simply by dividing the total cross section by the relative velocity of the Leonid meteors and the Earth. The brightness of the scattered sunlight is the product of this mean volume

scattering function, the solar flux, the length of the line of sight L, and the albedo A of the meteoroids [5]. Figure 3 shows the brightness as a function of α and χ for a maximum ZHR = 300, as observed in the Leonid outburst in 1998. The meteoric cloud is assumed to be resulted from an outburst of meteor stream activities associated with the return of P/Tempel-Tuttle. Based on the dynamical restrictions discussed above, we estimate the lower limit in the size integration to be 100 μm. It follows from Figure 3 that the observed cloud brightness cannot be explained by a simple power-law size distribution unless $\alpha \sim 0.4$ and $\chi \geq 3$. In high velocity streams such as Leonid, the luminosity I of a meteor could be proportional to the kinetic energy [20]. In this case, $I \sim M \sim 10^{-0.4*m}$ and consequently α equals 0.4. However, visual observations of the Leonid meteor stream in 1998 reported much lower values for χ (Arlt 1998). Furthermore, numerous meteoroids around 100 μm in size should have been detected as faint meteors by the video imaging instruments onboard the Leonid MAC mission [21]. Therefore, the size distribution and/or spatial density of meteoroids in the local volume swept by the Earth must be significantly different from the global average, provided that the meteoric cloud is directly related with the outburst of meteor stream activities.

The observed flux 2 $S_{10\odot}$ at the outermost lines in Figure 2 corresponds to a total scattering cross section density of 4.7e-22 cm^2/cm^3. If the meteoroids consist of spherical particles 100 μm in size, a spatial number density of 1.5e-18 /cm^3 leads to a huge discrepancy with the results from video imaging of faint meteors, as noted before. On the other hand, the critical value for bound orbits is derived as $\beta_c <= (1 - e_p)/2$ from eq.(2). Substituting $e_p = 0.906$ for P/Tempel-Tuttle, we obtain β_c= 0.047, which corresponds to approximately 4 μm meteoroids consisting of astronomical silicate. Thus, the typical size of meteoroids responsible for the cloud would be several tens of microns. If the typical size is 10μm and the albedo is 0.1, the number density is approximately 1.5e-16 $/cm^3$. Such meteoroids tend to accumulate at perihelion, as dispersion is negligible according to eq.(3), despite the significant increase in their orbital period. Such small meteoroids can be included in the diffuse and spatially uniform trail, which causes the annual activities of the meteor stream, and contribute to the observed brightness of the cloud.

In this case, we should be able to observe the Leonid cloud irrespective of the occurrence of outburst. Also, it is likely that meteoric clouds are also associated with other major meteor streams, such as the Perseid, Quadrantids, Orionids and Draconid, whose parent comets are far from perihelion.

REFERENCES

Arlt, R. 1998, WGN, Journal of the International Meteor Organization, 26, 239

Sykes M.V. & Walker R.G. 1992, *Icarus*, 95, 180 339

Nakamura, R. & Hidaka, Y. 1998, A&A, 340, 329

Brown, P. & Jones, J. 1998, *Icarus*, 133, 36

Richter, I., Leinert, C. and Planck, B. 1982,A&A, 110, 115

Ishiguro,M. et al. 1999, ApJ, 511, 432

Jenniskens, P. 1995,A&A, 295, 206

Yeomans,D.K. 1981, *Icarus*, 47, 492

Press et al. 1986, Numerical Recipes in C, Cambridge University Press.

Hong S.S., Kwon S.M., Park,Y.-S.& Park,C. 1998 *Earth, Planets and Space*, 50 , 487

Leinetr,Ch. et al. 1998, *Astron. Astrophys. Suppl.*, 127, 1

Dumont, R.1965 *Ann. Astrophys.* 28, 265 (English Transl., *NASA TT FII*, 164, 1965)

Van Rhijn, P.J. 1919, ApJ, 50, 356

Kelsall, T. et al. 1998, ApJ, 508,44

Hong, S. S. 1985, A&A, 146, 67

Smith, S. et al. 1999, Geophysical. Res. Lett., in press

Wu, Z. & Williams, I. P. 1996, MNRAS, 280, 1210

Mukai, T. 1985, A&A, 153, 213

Jenniskens, P. 1994, A&A, 287, 990 (1994)

Brown, P. et al. 1998, MNRAS, 300, 244

Jenniskens, P. 1999, Meteoritics and Planetary Science, in press

This manuscript was prepared with the AAS LaTeX macros v4.0.

Acknowledgements

This work is supported by a grant from the U.S. Air Force Office of Scientific Research. We thank members of the SUBARU project office in Hilo, Hawaii, for providing us with the opportunity to make observations on Mauna Kea.

Correspondence and requests for materials to Ryosuke Nakammura (ryosuke@kobe-u.ac.jp)

Figure legends

Figure 1

A model dust trail seen at 19:30 (UT) on 17th November 1998. The horizontal and vertical axes denote the solar elongation angle and the ecliptic latitude respectively. The trail is assumed to be a cylindrical tube with a radius of 0.01 astronomical unit along the orbit of comet P/Tempel-Tuttle. The cross denotes the location of the radiant.

Figure 2

Sky image taken at 15:04 UT on 17th November atop Mauna Kea, Hawaii. Contributions from integrated starlight and scattering by the lower atmosphere have been removed from the sky brightness, but the stars remain and the grid lines are drawn with the same intervals as in Figure 1 for comparison. The sky brightness, dominated by zodiacal light, increases towards the lower left corner as the solar elongation and ecliptic latitude decrease. After subtraction of the airglow continuum and zodiacal light, we show the residual component in the box at the upper left and superimpose a contour map with increments of 0.5 $S_{10\odot}$ on the meteoric cloud. Another bright spot in the box is the halo yielded by the bright star Zozca of Leo. It should be noted that the peak intensity of the meteoric cloud is only 4.5 $S_{10\odot}$, while the brightnesses of the zodiacal light amount to 200 $S_{10\odot}$ at the center of the image.

Figure 3

Expected cloud brightness in Log($S_{10\odot}$) for ZHR = 300, A = 0.1 and L = 0.3 AU. Note that the brightness is proportional to ZHR, A and L. The horizontal axis denotes the exponent in the mass-magnitude relation and the vertical axis is the population index determined from visual observations of meteors. The size distribution of meteoroids is assumed to follow eq.(4) in the text and the lower limit is set as 100 μm.

FIGURE 1

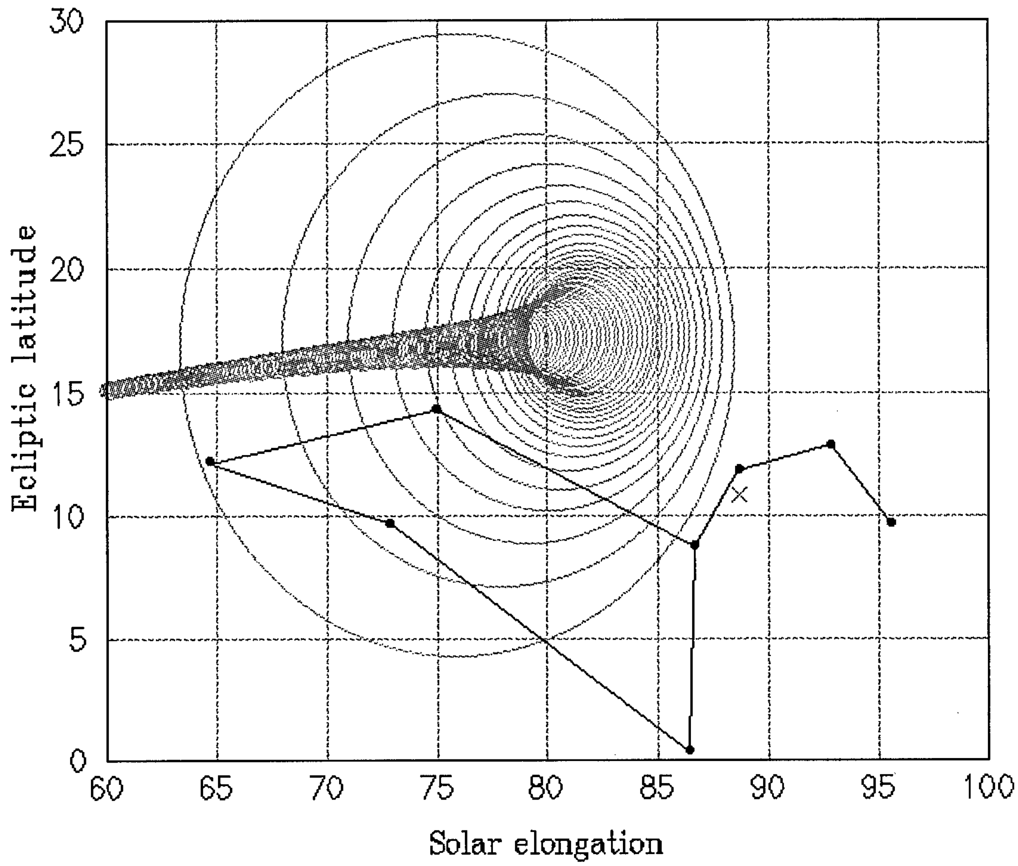

Correspondence to Ryosuke Nakammura (ryosuke@kobe-u.ac.jp)

FIGURE 2

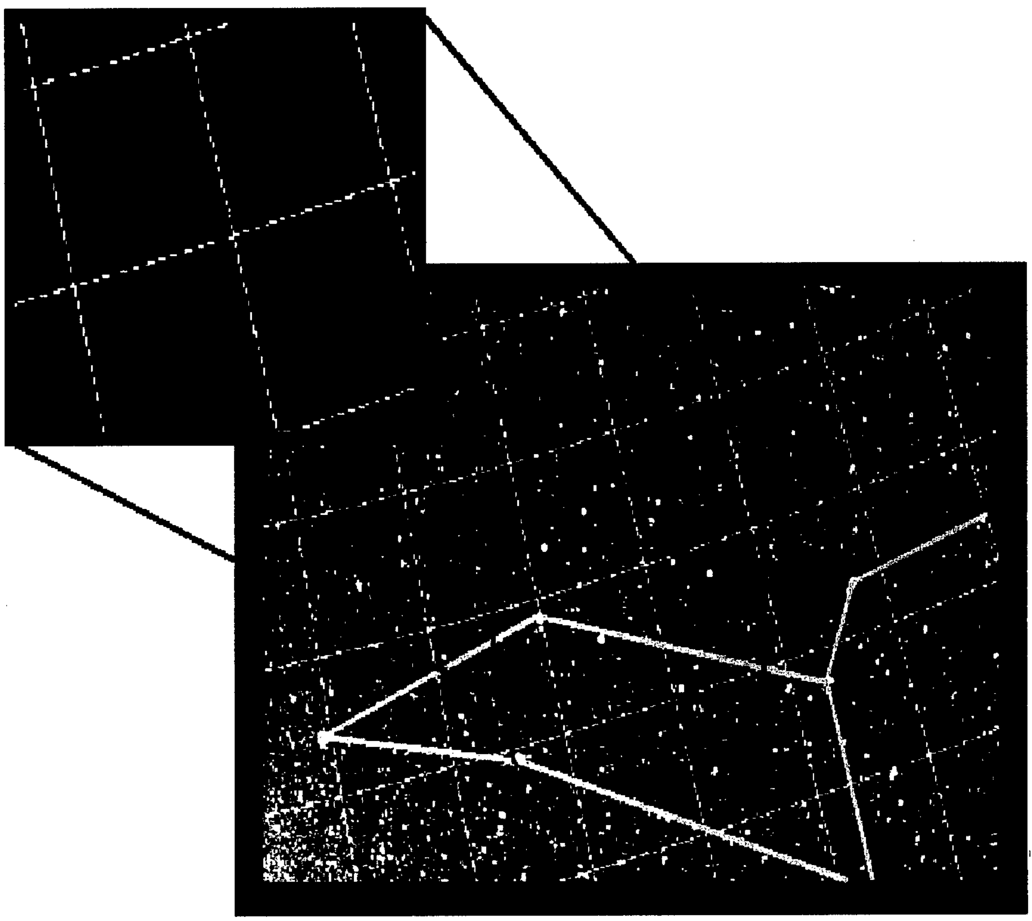

Correspondence to Ryosuke Nakammura (ryosuke@kobe-u.ac.jp)

FIGURE 3

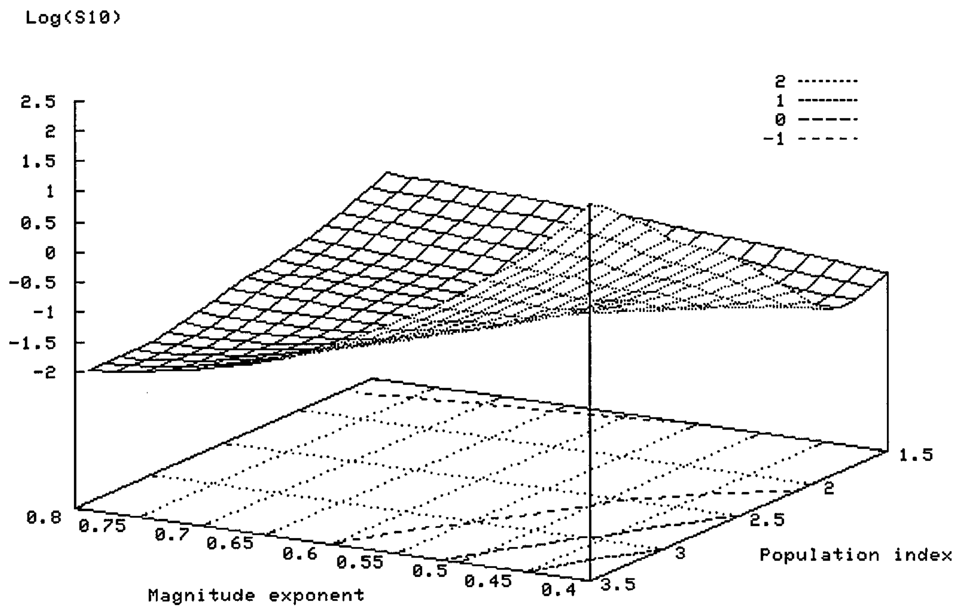

Correspondence to Ryosuke Nakammura (ryosuke@kobe-u.ac.jp)